Molecular Therapy
Original Article

Combined Antitumor Effects of Sorafenib and GPC3-CAR T Cells in Mouse Models of Hepatocellular Carcinoma

Xiuqi Wu,[1,4] Hong Luo,[1,2,4] Bizhi Shi,[1] Shengmeng Di,[1] Ruixin Sun,[1] Jingwen Su,[1] Ying Liu,[1] Hua Li,[1] Hua Jiang,[1] and Zonghai Li[1,3]

[1]State Key Laboratory of Oncogenes and Related Genes, Shanghai Cancer Institute, Renji Hospital, Shanghai Jiaotong University School of Medicine, Shanghai 200032, China; [2]State Key Laboratory of Oncogenes and Related Genes, Renji Hospital, School of Biomedical Engineering, Shanghai Jiao Tong University, Shanghai, China; [3]CARsgen Therapeutics, Shanghai 200032, China

Our previous study indicated that GPC3-targeted chimeric antigen receptor (CAR) T cell therapy has a high safety profile in patients with hepatocellular carcinoma (HCC). However, the response rate requires further improvement. Here, we analyzed the combined effect of GPC3-CAR T cells and sorafenib in both immunocompetent and immunodeficient mouse models of hepatocellular carcinoma. In immunocompetent mouse model, mouse CAR (mCAR) T cells induced regression of small tumors (approximately 130 mm^3 tumor volume) but had no effect on large, established tumors (approximately 400 mm^3 tumor volume). Sorafenib, at a subpharmacologic but not a pharmacologic dose, augmented the antitumor effects of mCAR T cells, in part by promoting IL12 secretion in tumor-associated macrophages (TAMs) and cancer cell apoptosis. In an immunodeficient mouse model, both subpharmacologic and pharmacologic doses of sorafenib had limited impacts on the function of human CAR (huCAR) T cells *in vitro* and showed synergistic effects with huCAR T cells *in vivo*, which can at least partially be ascribed to the upregulated tumor cell apoptosis induced by the combined treatment. Thus, this study applied two of the most commonly used mouse models for CAR T cell research and demonstrated the clinical potential of combining sorafenib with GPC3-targeted CAR T cells against HCC.

INTRODUCTION

Chimeric antigen receptors (CARs) are engineered receptors with an extracellular, antigen-specific, single-chain variable fragment (scFv) fused with intracellular T-cell-activating and costimulatory signaling domains.[1] T cells isolated from patients are activated and genetically engineered to express CARs to mediate non-major histocompatibility complex (MHC)-restricted killing of tumor cells. To date, CAR T cell therapy has shown demonstrable success against hematologic malignancies: for example, CD19 CAR T cells against lymphoid leukemia and B-cell maturation antigen (BCMA) CAR T cells against multiple myeloma.[2–5] However, therapeutic application of CAR T cell therapy against solid tumors has been much less promising.[6,7] Our phase I clinical trial (ClinicalTrials.gov: NCT02395250) in 13 Chinese patients showed partial antitumor activity in patients with hepatocellular carcinoma (HCC), but the response needs further improvement.[8] It is well known that the hostile immunosuppressive microenvironment within HCC is a key barrier to the antitumor efficacy of CAR T cell therapy.[9–11] In addition, one strategy to overcome this hostile environment is a combination of CAR-T cells with antitumor compounds or immune-modulatory agents.[12–14]

Sorafenib, an orally administered multikinase inhibitor, is currently the most widely used drug for advanced HCC.[15] Sorafenib exhibits pro-apoptotic and antiangiogenic effects by inhibiting multiple kinases, including Raf kinase, vascular endothelial growth factor receptor, platelet-derived growth factor receptor, KIT, FLT-3, and RET tyrosine kinases.[16–18] It has also been reported that sorafenib has immune-modulatory effects, although these studies may seem contradictory. On one hand, several groups have shown that sorafenib exerts immunosuppressive effects by directly impairing the activation of human peripheral blood T cells.[19,20] Sorafenib treatment also increased intratumoral hypoxia, which resulted in immunosuppressive actions, including increased intratumoral expression of programmed death (PD) ligand-1 and accumulation of regulatory T cells (Tregs) and M2-type macrophages.[21] On the other hand, it has also been shown that sorafenib can reduce the number of PD-1^+ T cells and Tregs in HCC patients and mouse models[22,23] and can modulate the macrophage cytokine phenotype toward an immunosupportive profile, which promotes the functions of immune effector cells.[24–26]

Received 27 January 2019; accepted 23 April 2019;
https://doi.org/10.1016/j.ymthe.2019.04.020.

[4]These authors contributed equally to this work.

Correspondence: Zonghai Li, State Key Laboratory of Oncogenes and Related Genes, Shanghai Cancer Institute, Renji Hospital, Shanghai Jiaotong University School of Medicine, Shanghai 200032, China.
E-mail: zonghaili@163.com
Correspondence: Hua Jiang, State Key Laboratory of Oncogenes and Related Genes, Shanghai Cancer Institute, Renji Hospital, Shanghai Jiaotong University School of Medicine, Shanghai 200032, China.
E-mail: jianghuapy@163.com

Considering its antitumor activities and potential capacity to modulate the tumor microenvironment, sorafenib has been applied to improve the efficacy of several immunotherapy drugs, such as monoclonal antibodies, tumor vaccines, and immune checkpoint inhibitors.[26–28] In this study, we explored the possible combination of sorafenib with GPC3-targeted CAR T cells in both immunocompetent and immunodeficient mouse models of HCC. The underlying mechanism of their combined effect was also elucidated.

RESULTS

Mouse CAR T Cells Failed to Control Large, Established Hepatocellular Tumors in Immunocompetent Mice

To better understand the effect of the microenvironment on CAR-T cell antitumor activities, C57BL/6 mice bearing murine Hepa1-6-chGPC3 tumor xenografts were established. Hepa1-6-chGPC3 cells were constructed by transfecting Hepa1-6 cells with chGPC3, which was a human-mouse GPC3 chimera containing the binding epitope of an anti-human GPC3 antibody (9F2) (Figure 1A). The transfectants were recognized by 9F2 antibodies (Figure 1B). Splenic T cells from C57BL/6 mice were genetically engineered with a 9F2-m28z CAR composed of 9F2 scFv linked to mouse CD28 and CD3z endodomains (Figures 1C and 1D; Figure S1A). The basic phenotypes (CD3/CD4/CD8) of mCAR T cells are provided in Figure S2A. On days 4 and 9 after subcutaneous injection of Hepa1-6-chGPC3 tumor cells, the indicated T cells were administered to mice with small or large tumors (approximately 130 or 400 mm^3 in tumor volume, respectively) (Figure 1E). Tumor growth and survival were monitored for 60 days. Compared with untransduced (UTD) T cells, GPC3-targeted mCAR T cells significantly inhibited tumor growth and increased survival of the mice with initially small tumors. However, mCAR T cells failed to control tumor growth and failed to extend the survival of the mice with initially large tumors (Figures 1F and 1G).

A Pharmacologic but Not a Subpharmacologic Sorafenib Concentration Inhibits Antigen-Induced mCAR T Cell Responses *In Vitro*

Since we do not know whether sorafenib, a multikinase inhibitor, can inhibit kinases involved in T cell activation, the impact of sorafenib on mCAR T cells *in vitro* was investigated. In the presence of sorafenib and tumor cells, antigen-induced expression of the antitumor cytotoxicity marker CD107a and interferon-γ (IFN-γ) was decreased in mCAR T cells, and this decrease became especially significant when a pharmacologic dose (10 μM) of sorafenib was used (Figure 2A). Similar inhibitory trends regarding the proliferation (Figure 2B) and cytotoxic activity (Figure 2C) of mCAR T cells after antigen stimulation and sorafenib exposure were also observed. Cytokine secretion by mCAR T cells in response to target antigen was also measured in the presence of different concentrations of sorafenib. At 1 μM, sorafenib increased the secretion of IL-2 (Figure 2D) but showed limited effect on the secretion of IFN-γ (Figure 2E) and TNF-α (Figure 2F). However, significant decreases in IL-2, IFN-γ, and TNF-α production by mCAR T cells were observed in the presence of 10 μM sorafenib (Figures 2D–2F).

Subpharmacologic Doses of Sorafenib Enhance the Therapeutic Efficacy of mCAR T Cells *In Vivo*

To further investigate whether a functional synergism between sorafenib and GPC3-mCAR T cells occurs *in vivo*, mice bearing large Hepa1-6-chGPC3 tumors were administered sorafenib at a subpharmacologic dose (7.5 mg/kg per day) or pharmacologic dose (30 mg/kg per day) from days 8 to 18 and treated with GPC3-mCAR T cells on days 9 and 13 (Figure 3A). Tumor growth and survival were observed for 2 months. Compared with other treatments, mCAR T cell treatment in combination with sorafenib at the subpharmacologic dose led to the strongest tumor growth inhibition, resulting in significantly smaller tumors, with volumes (mean [SD]) of CAR+vehicle versus CAR+Sora7.5 (1,764.3 [191.4] mm^3 versus 794.5 [123.5] mm^3; $p < 0.001$; Figure 3B) and longer survival times of the mice (Figure 3C). In addition, the infiltration of mCAR T cells in tumor tissues was analyzed via flow cytometry on day 11. GPC3-mCAR T cells combined with the subpharmacologic dose of sorafenib resulted in increased mCAR T cell infiltration and a higher percentage of CAR^+ IFN-γ^+ T cells in tumor tissues compared with mice that received mCAR T cells alone or mCAR T cells plus the pharmacologic dose of sorafenib (Figures 3D–3F).

We also tested the effect of mCAR T cells combined with the subpharmacologic dose of sorafenib in mice bearing moderate-sized Hepa1-6-chGPC3 tumors (approximately 200 mm^3 in tumor volume). Sorafenib (7.5 mg/kg per day) or vehicle was orally administered beginning on day 6 for 5 consecutive days, and 2×10^6 mCAR T cells or UTD T cells were injected intravenously on day 7 after tumor cell inoculation (Figure 3G). Single administration of mCAR T cells or sorafenib and combined administration of UTD T cells and low-dose sorafenib had a moderate inhibitory effect on tumor growth, whereas responses were significantly improved after combined use of mCAR T cells and low-dose sorafenib, with tumor volumes of CAR+vehicle versus CAR+sorafenib (407 [96.0] mm^3 versus 19.5 [16.8] mm^3; $p < 0.05$; Figure 3H). Mice were sacrificed on day 28. Tumor weights were measured and were in accordance with tumor volumes (Figures S3A and S3B). Tumor tissues in the CAR T cell-treated group still had chGPC-3 expression and T cell infiltration, as observed by immunohistochemical (IHC) staining (Figures S4, S5A, and S5B). The higher amount of T cells in the CAR T cell-treated groups (CAR T and their combination with sorafenib) compared with the other control groups suggesting the persistence of the CAR T cells in the tumor tissues. Taken together, these data show that lower- but not pharmacologic-dose sorafenib treatment enhanced the antitumor efficacy of mCAR T cell therapy in an immunocompetent mouse model.

Sorafenib-Treated Macrophages Enhance mCAR T Cell Activity by Upregulating IL12 Production

Previous studies have shown that sorafenib can modulate the expression of IL12 in macrophages and can exhibit an immune stimulatory function.[24–26] To study whether this immunoregulation effect of sorafenib contributes to the improved antitumor activity of GPC3-mCAR T cells, IL12 expression in tumor tissues after treatment with subpharmacologic doses of sorafenib or vehicle was examined.

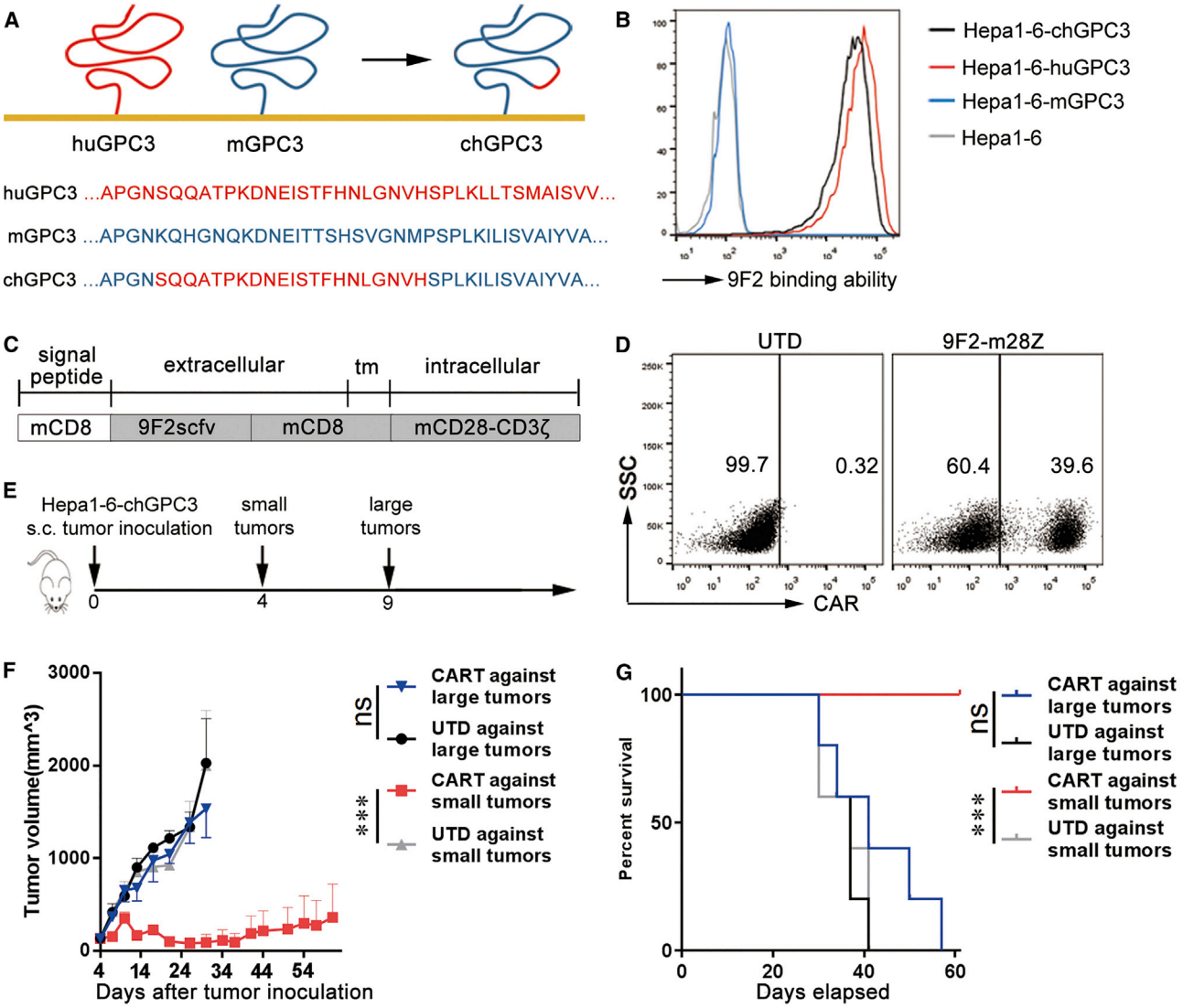

Figure 1. GPC3-mCAR T Cells Have Poor *In Vivo* Efficacy against Large Tumors in Immunocompetent Mice

(A) Construction of chGPC3. Amino acids 538–558 in mGPC3 were replaced with the huGPC3-derived 9F2-binding epitope (^{539}SQQATPKDNEISTFHNLGNVH^{559}). (B) Overexpression of chGPC3 in Hepa1-6 cells. mAb 9F2 did not recognize mGPC3 but showed binding affinity comparable to huGPC3 and chGPC3 overexpressed in Hepa1-6 cells. (C) Schematic diagram of the modular composition of GPC3-CAR. 9F2scFv, GPC3-specific single chain (heavy and light) fragment variable; tm, transmembrane domain; mCD28-CD3ζ, combined intracellular mouse CD28 and CD3ζ signaling domain. (D) Modified T cells expressed the CAR on the surface, determined by flow cytometry. (E) Experimental scheme. Hepa1-6-chGPC3 cells (1×10^7) were subcutaneously injected into C57BL/6 mice. Mice with small tumors (day 4) or large tumors (day 9) received an i.v. injection of 2×10^6 GPC3-CAR T cells. (F and G) The average tumor growth (F) and survival (G) curves of each treatment group are shown (n = 5). The results are expressed as the mean ± SEM. Significance of findings was defined as follows: ns, not significant; $p > 0.05$; *$p < 0.05$; **$p < 0.01$; ***$p < 0.001$.

The expression levels of IL12 mRNA in tumor-associated macrophages (TAMs) and IL12 protein within the tumor microenvironment were significantly increased in the sorafenib-treated group (Figures 4A and 4B). In addition, we observed IL12 upregulation in lipopolysaccharide (LPS)-activated bone marrow-derived macrophages (BMDMs) induced by 1–5 μM sorafenib (Figure 4C). However, BMDMs treated with 10 μM sorafenib showed no significant change in the IL12 expression level (Figure 4C), mainly as a result of the dose-dependent cytotoxicity of sorafenib in response to LPS-activated BMDMs (Figure 4D). To confirm whether sorafenib-treated BMDMs enhance the activity of GPC3-mCAR T cells, BMDMs were Transwell-cultured with Hepa1-6-chGPC3 and mCAR T cells in the presence of LPS and various concentrations of sorafenib (Figure 4E). In this coculture system, low-concentration (1–5 μM) sorafenib but not 10 μM sorafenib increased the IFN-γ production of mCAR T cells in the presence of LPS-stimulated BMDMs (Figure 4E).

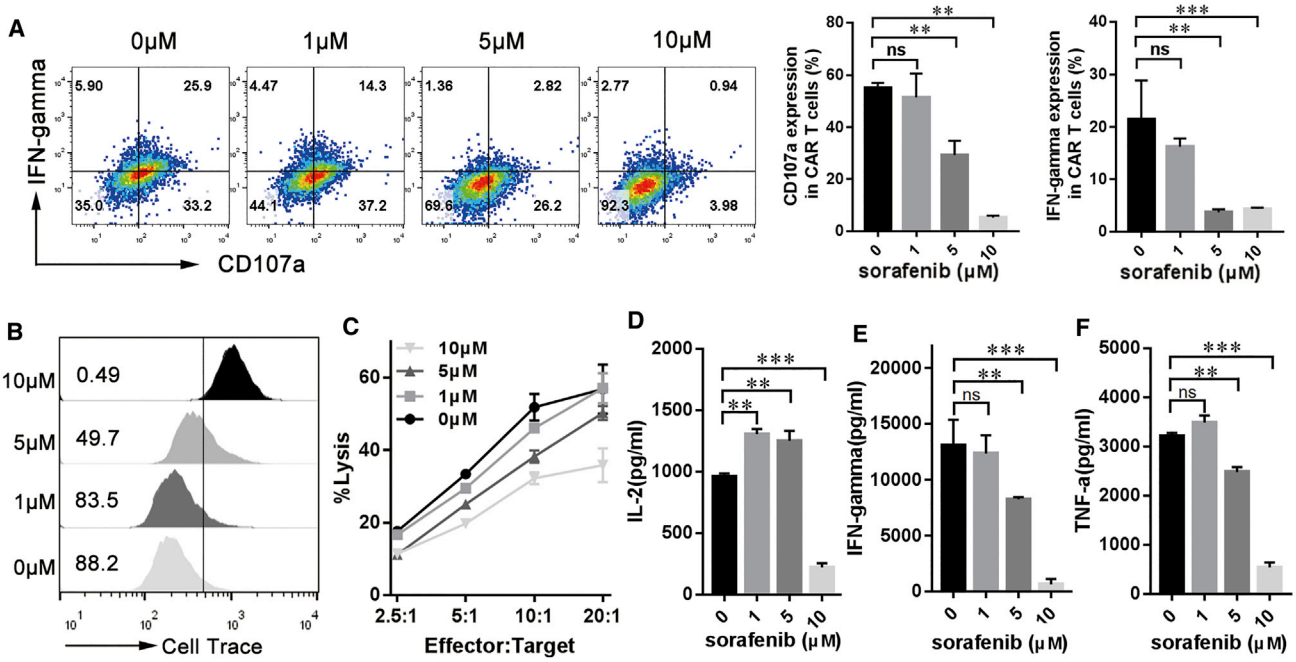

Figure 2. High-Dose, but Not Low-Dose, Sorafenib Inhibits the Function of GPC3-mCAR T Cells *In Vitro*

(A) Sorafenib inhibits CD107a expression and IFN-γ production in mouse CAR T cells. GPC3-mCAR T cells (1×10^5 cells per well) were stimulated with Hepa1-6-chGPC3 at a 1:1 ratio in the presence of 1, 5, or 10 μM sorafenib for 24 h. After cell surface and intracellular staining, the percentages of mCAR T cells expressing the relevant markers was determined via multicolor flow cytometry. (B) Sorafenib inhibits mCAR T cell proliferation. GPC3-mCAR T cells were labeled with Cell Trace Violet, and then, 1×10^5 Cell Trace–labeled mCAR T cells were incubated with 1×10^5 Hepa1-6-chGPC3 cells in the presence of various concentrations of sorafenib for 24 h. The number of gated cells indicate the dividing cell population. (C) Reduced cytotoxicity was observed after incubation of sorafenib-pretreated mCAR T cells with Hepa1-6-chGPC3 cells at various effector:target (E:T) ratios for 4 h, determined by a standard nonradioactive cytotoxic assay. (D–F) *In vitro* cytokine production of mCAR T cells. Briefly, 1×10^5 mCAR T cells were cultivated in 24-well plates precoated with GPC3 protein. After 24 h, culture supernatants were harvested and assayed for IL-2 (D), IFN-γ (E), and TNF-α (F) via cytometric bead array (CBA). All data are presented as the mean ± SEM of triplicate experiments. Significance of findings was defined as follows: ns, not significant; $p > 0.05$; *$p < 0.05$; **$p < 0.01$; ***$p < 0.001$.

Furthermore, blocking experiments with IL12 antibody confirmed IL12 as a sorafenib-triggered mCAR T cell stimulus (Figure 4F).

Human PBMC- and Mouse Spleen-Derived CAR T Cells Have Different Sensitivities to Sorafenib

We next asked whether the antitumor activity of human peripheral blood mononuclear cell (PBMC)-derived CAR (huCAR) T cells against human live cancer could also be improved by sorafenib. First, human PBMCs were activated and transduced with 9F2-hu28z CAR (Figures 5A and 5B; Figure S1B). The basic phenotypes (CD3/CD4/CD8) of huCAR T cells are provided in Figure S6A. *In vitro* activities of huCAR T cells were further analyzed in the presence of various concentrations of sorafenib. We found that both pharmacologic and subpharmacologic concentrations of sorafenib had no significant influence on the CD107a expression (Figure 5C), proliferation (Figure 5D), or cytotoxicity (Figure 5E) of huCAR T cells. Moreover, sorafenib upregulated the IL-2 production of huCAR T cells in a dose-dependent manner (Figure 5F) and had a limited impact on IFN-γ (Figure 5G) and TNF-α (Figure 5H) secretion. Compared with huCAR T cells, dramatic decreases in CD107a expression and IL-2, IFN-γ, and TNF-α production were observed in mCAR T cells in the presence of 10 μM sorafenib (Figure 5I). These results indicate that mouse spleen- and human PBMC-derived CAR T cells have different sensitivities to high-dose sorafenib.

Sorafenib Treatment Enhances the Efficacy of Human CAR T Cells against HCC in Immunodeficient Mice

To test the combination effect of sorafenib and huCAR T cells *in vivo*, a xenograft tumor model was established with $GPC3^+$ PLC/PRF/5 cells in NOD/Scid $IL2R\gamma C^{null}$ (NSG) mice. On day 11 after transplantation, the mice were treated with one dose of 2×10^6 huCAR T cells plus a low (7.5 mg/kg) or high (30 mg/kg) daily dose of sorafenib for 2 consecutive weeks (Figure 6A). The dosage of huCAR T cells used in this experiment was lower than that in our previous study.[29] Both the pharmacologic and subpharmacologic doses of sorafenib combined with huCAR T cells synergistically reduced tumor growth compared to monotherapies, with tumor volumes of CAR+vehicle versus CAR+Sora7.5 of 1,326.1 (186.2) mm^3 versus 557.1 (113.5) mm^3 ($p < 0.001$) and tumor volumes of CAR+vehicle versus CAR+Sora30 of 1,326.1 (186.2) mm^3 versus 440.3 (203.6) mm^3 ($p < 0.001$; Figure 6B). The tumor growth suppression effect caused by the combination treatment was further confirmed by the reduced tumor weight in

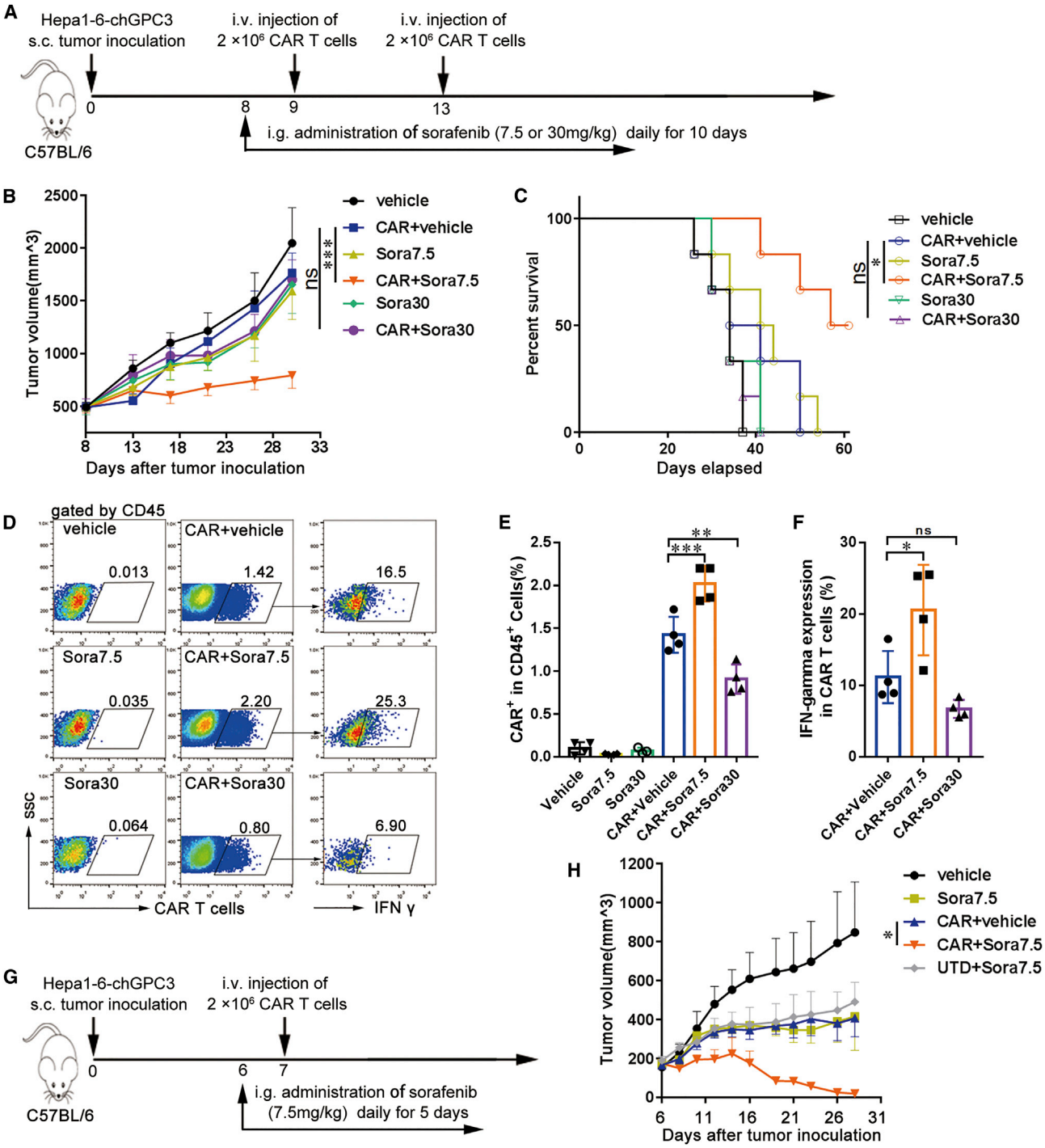

Figure 3. A Subpharmacologic Dose of Sorafenib Augments the Antitumor Activity, Infiltration, and Cytokine Production of GPC3-mCAR T Cells *In Vivo*

(A) *In vivo* experimental design. Hepa1-6-chGPC3 tumor cells (1×10^7) were subcutaneously injected into C57BL/6 mice and allowed to establish for 8 days. Mice were assigned to six experimental groups as indicated, vehicle or sorafenib at 7.5 (Sora7.5) or 30 (Sora30) mg/kg was administered via gavage for 10 days, and 2×10^6 GPC3-mCAR T cells were adoptively transferred i.v. on days 9 and 13. (B and C) Tumor growth (B) and survival (C) curves of treatment groups (n = 6). (D) Representative flow cytometry plots showing the frequencies of Cell Trace Violet prelabeled mCAR T cells in tumor-infiltrating $CD45^+$ cells (E) and IFN-γ^+ cells in mCAR T cells (F) on day 11 (n = 4). (G) Treatment protocol. Six days after tumor inoculation, mice were divided into five experimental groups, as indicated, and then treated with 7.5 mg/kg (Sora7.5) sorafenib for 5 days. Then, 2×10^6 mCAR or untransduced (UTD) T cells were injected i.v. on day 7. (H) Tumor growth curves (n = 6). The results are expressed as the mean ± SEM. Significance of findings was defined as follows: ns, not significant; $p > 0.05$; *$p < 0.05$; **$p < 0.01$; ***$p < 0.001$.

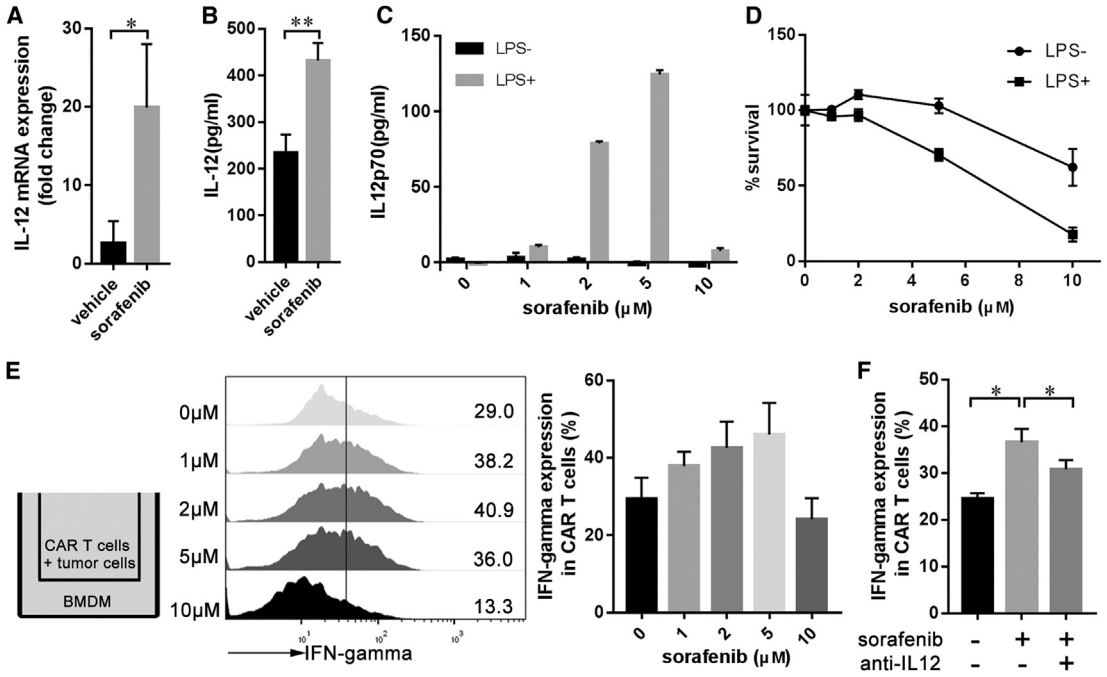

Figure 4. A Subpharmacologic Dose of Sorafenib Triggers mCAR T Cell Activation in the Presence of Macrophages

(A and B) Expression levels of IL12 mRNA in TAMs (A) and IL12 protein in the TME (B). Eight days after Hepa1-6-chGPC3 tumor implantation, mice were treated with vehicle or 7.5 mg/kg sorafenib for 5 days. On day 14, tumors were harvested for further detection (n = 3). TAMs were isolated with anti-F4/80 microbeads, and IL12 mRNA in TAMs was evaluated via qPCR (n = 3). Tumor lysates were assayed for IL12 via ELISA. (C) Sorafenib triggered IL12 secretion in BMDMs. BMDMs were treated with different concentrations of sorafenib and LPS (10 ng/mL) for 24 h. IL12 secretion into culture supernatants was assayed via ELISA. The data are representative of three independent experiments. (D) Cytotoxicity of sorafenib to BMDMs. The cell viability of BMDMs was shown after treatment with the indicated concentrations of sorafenib in the presence or absence of LPS (10 ng/mL) for 24 h. The data are representative of three independent experiments. (E) Transwell coculture of mCAR T cells with BMDMs. BMDMs were treated with sorafenib and LPS (10 ng/mL) for 8 h. Then, mCAR T cells and tumor cells were added to the upper chamber for another 16 h for coculture with sorafenib-treated BMDMs. IFN-γ expression in mCAR T cells was assayed by flow cytometry. (F) Blocking experiment. Sorafenib (2 μM) and anti-IL12 antibody (5 μg/mL) were added to the coculture system as mentioned in (E). Each data point reflects the mean ± SEM of triplicate experiments. Significance of findings was defined as follows: ns, not significant; $p > 0.05$; *$p < 0.05$; **$p < 0.01$; ***$p < 0.001$.

the combination treatment group compared with that in other treatment groups (Figure 6C). The infiltration of huCAR T cells in PLC/PRF/5 xenografts was further determined by IHC staining at the endpoint. Mice treated with huCAR T cells plus sorafenib (7.5 or 30 mg/kg) exhibited increased huCAR T cell accumulation in tumor tissues compared with mice treated with huCAR T cells only (Figures 6D and 6E). There was no specific staining in the groups without huCAR T cell treatment (Figures 6D and 6E). These results indicate that both subpharmacologic and pharmacologic doses of sorafenib had synergistic antitumor effects with huCAR T cells.

NSG mice are highly immunodeficient and lack mature T cells, B cells, and natural killer cells and have many defects in macrophages and dendritic cells.[30] Furthermore, mouse macrophages did not increase the function of huCAR T cells in the presence of sorafenib *in vitro* (Figure S7). Therefore, in NSG mice, sorafenib should enhance the antitumor activities of huCAR T cells in a macrophage-independent manner. As sorafenib is known to induce apoptosis in HCC cells, we hypothesized that sorafenib could sensitize tumor cells to huCAR-T-cell-mediated killing. Cleaved caspase-3 staining of PLC/RPF/5 xenograft sections showed that tumor cell apoptosis was significantly increased when sorafenib and huCAR T cells were combined (Figures 6F and 6G). A similar effect was observed in PLC/RPF/5 cells treated with sorafenib and huCAR T cells *in vitro*, according to Annexin V staining (Figures 6H and 6I). Furthermore, the apoptosis-inducing effect of sorafenib and mCAR T cell treatment on Hepa1-6-chGPC3 cells was examined. Sorafenib at 5 μM but not at the pharmacologic concentration (10 μM) exhibited the most significant apoptosis-inducing effect on Hepa1-6-chGPC3 cells with mCAR T cell treatment (Figure S8), suggesting that sorafenib enhances the antitumor efficacy of mCAR T cells through both macrophage modulation and apoptosis promotion.

DISCUSSION

To date, a series of clinical trials of CAR T cell therapy have shown demonstrable success in hematologic malignancies, including acute lymphoid leukemia, chronic lymphoid leukemia, and multiple myeloma.[2–5,31] However, similar success has not been observed in CAR T cell trials for solid tumors.[6,7] In this study, we found that

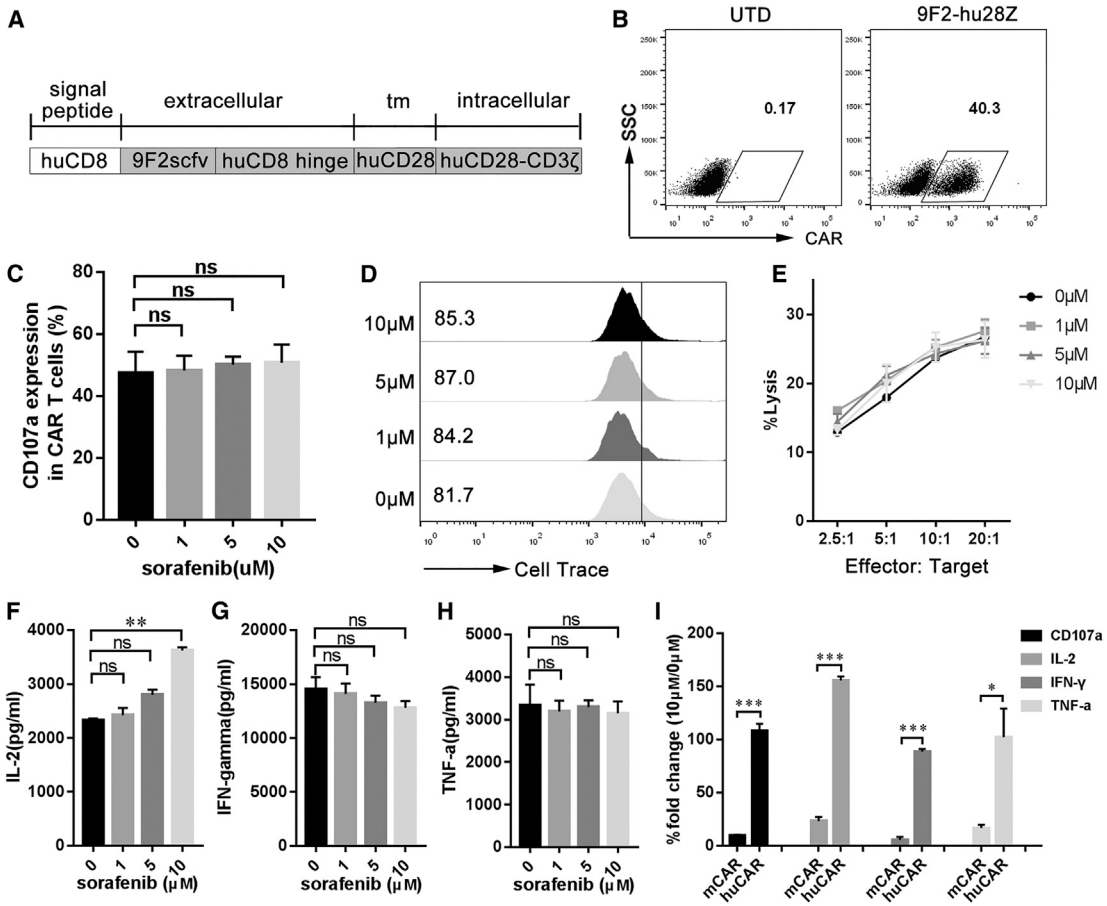

Figure 5. Sorafenib Has No Significant Effect on the Activity of huCAR T Cells *In Vitro*

(A) Schematic representation of the modular composition of GPC3-specific human CAR. 9F2scFv, GPC3-specific single chain (heavy and light) fragment variable; tm, transmembrane domain; huCD28-CD3ζ, combined intracellular human CD28 and CD3ζ signaling domain. (B) Modified T cells express 9F2-hu28z CAR on their surface, based on flow cytometry results. (C) CD107a expression in activated huCAR T cells in the presence of sorafenib. huCAR T cells were stimulated with PLC/PRF/5 cells at 1:1 ratio in the presence of 1, 5, or 10 μM sorafenib for 24 h. Then, CD107a expression in huCAR T cells was assayed by flow cytometry. (D) The effect of sorafenib on huCAR T cell proliferation. huCAR T cells were prelabeled with Cell Trace Violet dye and then incubated with PLC/PRF/5 cells at a 1:1 ratio in the presence of different concentrations of sorafenib for 48 h. The numbers gated indicate the dividing cell population. (E) Cytotoxicity of sorafenib-pretreated huCAR T cells against tumor cells. huCAR T cells were pretreated with various concentrations of sorafenib for 4 h and then cocultured with PLC/PRF/5 cells at varying effector:target (E:T) ratios for 4 h for cytotoxic assays using a standard nonradioactive cytotoxic assay kit. The data are representative of three independent experiments. (F–H) *In vitro* cytokine production of huCAR T cells. Briefly, 1×10^5 huCAR T cells were cultivated in 24-well plates precoated with GPC3 protein. After 24 h, culture supernatants were harvested and assayed for IL-2 (F), IFN-γ (G), and TNF-α (H) via cytometric bead array (CBA). (I) Comparison of the activities (CD107a, IL-2, IFN-γ, and TNF-α) of mCAR and huCAR T cells after treatment with 10 μM sorafenib. All data are presented as the mean ± SEM of triplicate experiments, unless otherwise noted. Significance of findings was defined as follows: ns, not significant; $p > 0.05$; *$p < 0.05$; **$p < 0.01$; ***$p < 0.001$.

mouse GPC3-CAR T cells could eradicate small tumors effectively but failed to control large, established tumors. Baseline tumor size has been considered an independent prognostic factor for immunotherapy.[32] Other barriers, such as poor trafficking, antigen heterogeneity, and the immunosuppressive microenvironment within solid tumors, may also contribute to the non-satisfactory performance of CAR T cells in solid tumors. To address these obstacles in solid tumors, several corresponding strategies were proposed, including introducing chemokine receptors into CAR T cells,[33] the use of tandem CAR T cells for targeting of multiple antigens,[34] and combination with immune-regulating agents (T. Le Trinh et al., 2016, Am. Assoc. Cancer Res., abstract).[13]

Sorafenib, a multikinase inhibitor widely used for HCC, holds great promise for combination with GPC3-CAR T cell therapy. Sorafenib inhibits multiple cell surface tyrosine kinases and downstream intracellular serine/threonine kinases that are involved in tumor cell proliferation, apoptosis, and angiogenesis.[18] It has also been reported that sorafenib has multiple immune-modulatory effects. For instance, sorafenib can promote an antitumor immune response by enhancing

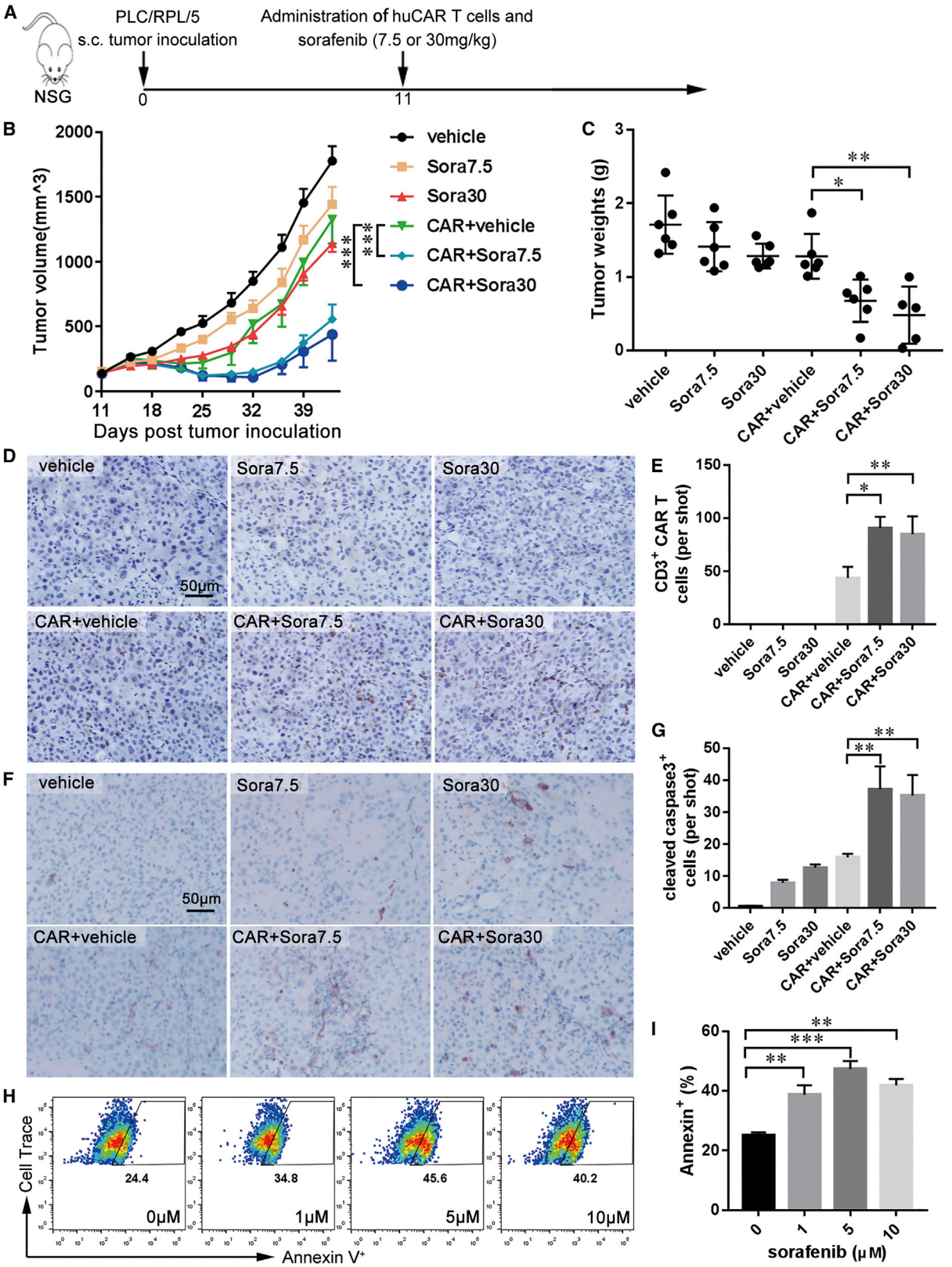

(legend on next page)

function of tumor-specific effector T cells, thus reducing the number of immunosuppressive cells and triggering the proinflammatory activity of TAMs.[22,23,25,26] Therefore, sorafenib has been used to enhance the therapeutic efficacy of adoptive transferred T cells and tumor-targeted vaccines.[26,35] However, in contrast, studies have postulated that sorafenib can directly inhibit activation of human peripheral blood T cells and has a detrimental effect on the immunostimulatory capacity of dendritic cells.[20,36] Considering the immunosuppressive and supportive effects of sorafenib, the optimal dose sought may offer the best synergistic benefit for combination with CAR T cells.

Pharmacokinetic studies of sorafenib in patients with HCC showed that the mean plasma concentration of sorafenib at 400 mg twice daily (the U. S. Food and Drug Administration [FDA]-recommended dose) was between 3 and 10 mg/L (approximately 5–16 μM).[37–39] Pharmacokinetic studies in mice also demonstrated that the mean plasma concentration of sorafenib administered at 30 mg/kg in mice was approximately 8 μM, which is similar to that in sorafenib-treated patients.[40,41] According to these studies, we used sorafenib at 10 μM *in vitro* and 30 mg/kg in mice to represent the pharmacologic dose and at 1 μM *in vitro* and 7.5 mg/kg in mice to represent a subpharmacologic dose. In our mCAR T cell experiments, the pharmacologic dose of sorafenib suppressed the proliferation, cytokine production, and cytotoxicity of mCAR T cells *in vitro* and showed no synergistic effect with GPC3 mCAR T cells against C57BL/6 HCC model mice. However, the subpharmacologic dose of sorafenib showed a limited impact on mCAR T cell functions and enhanced the therapeutic efficacy of mCAR T cells, in part by modulating the production of IL12 in TAMs. In our huCAR T cell experiments, we found that neither the pharmacologic nor the subpharmacologic dose of sorafenib had a significant influence on the functions of huCAR T cells *in vitro*, and at both doses, sorafenib synergized with huCAR T cells to improve antitumor efficacy *in vivo*. Thus, we propose that we can combine mCAR T cells with a subpharmacologic dose of sorafenib in immunocompetent mice for scientific research and combine huCAR T cells with pharmacologic doses of sorafenib in patients for clinical treatment.

The most commonly used mouse models for CAR T cell research are of two types: mouse spleen-derived CAR T cells against murine tumors in immunocompetent mice and human PBMC-derived CAR T cells against human tumor xenografts in immunodeficient mice.[29,33] The advantage of the immunocompetent mouse model for CAR T research is that the intact immune microenvironment within murine tumors is convenient for the study of interactions between mCAR T cells and other immune cell populations. The human CAR (huCAR) T cell therapeutic model in immunodeficient mice lacks an intact tumor immune microenvironment but more closely reflects the way the therapy is applied clinically. Both the immunocompetent and immunodeficient mouse models have unique advantages and were therefore used in this study. In the mCAR T cell therapeutic model experiments, we focused on the immune-regulatory effects of sorafenib and found that sorafenib induced IL12 secretion in macrophages and subsequently improved mCAR T cell activity. However, in our huCAR T cell studies in immune-compromised NSG mice, we found that sorafenib synergistically promoted HCC cell apoptosis with huCAR T cells and enhanced the antitumor efficacy of huCAR T cells. A synergistic effect on apoptosis induction was also observed between mCAR T cells and sorafenib against murine HCC cells. These results indicate that combining sorafenib with CAR T cell therapy increased treatment efficacy against HCC and that multiple mechanisms may be involved in the synergistic effect between sorafenib and CAR T cells.

Different sensitivities to high-dose sorafenib were observed between mouse and huCAR T cells in this study. The major reason for this difference may be the different origin of mouse and huCAR T cells. mCAR T cells were derived from mouse spleen and huCAR T cells from human PBMCs. Species difference may be the other reason. Additionally, mCAR T cells are much more sensitive to activation-induced cell death and have much shorter persistence than huCAR T cells.[42] Considering the difference between the behaviors of mouse and huCAR T cells, research results obtained from mCAR T cells should be reconfirmed in huCAR T cells.

Lymphodepletion before CAR T cell infusion is an important component of CAR T cell therapy.[43] In our phase I clinical trial of GPC3-CAR T cells against HCC, all six patients without lymphodepleting conditions who received CAR T cell therapy developed progressive disease. Among the seven patients with lymphodepleting conditions, one had a partial response, and two had stable disease.[8] One reason for the benefits of lymphodepletion is the elimination of Tregs by chemotherapeutic drugs before CAR T cell infusion.[44] Sorafenib has also been shown to reduce Tregs in HCC patients.[22] Hence, when we combine sorafenib and CAR T cell treatment in the clinic, lymphodepletion may also be considered as a beneficial part of a clinical treatment plan.

In summary, we established immunocompetent and immunodeficient mouse HCC models for GPC3-CAR T cell research and then

Figure 6. Combination of Sorafenib with huCAR T Cells Leads to Enhanced Antitumor Efficacy in NSG Mice

(A) *In vivo* experimental design. NSG mice were subcutaneously inoculated with 5×10^6 PLC/PRF/5 cells on day 0. On day 11, 2×10^6 huCAR T cells were intravenously administered, and vehicle or sorafenib at 7.5 mg/kg (Sora7.5) or 30 mg/kg (Sora30) was administered orally for 2 weeks. (B) Tumor growth curves (n = 5 or 6). (C) On day 43 after tumor cell inoculation, the mice were euthanized. Tumor weight was measured (n = 5 or 6). (D and E) Representative immunostaining images (D) and quantification (E) of huCAR T cell infiltration in tumor tissues (n = 5). Scale bars, 50 μm. (F and G) Immunohistochemistry analysis of activated caspase-3 in PLC/PRF/5 xenografts. Representative immunostaining images (F) and quantification (G) of activated caspase-3 in tumor tissues (n = 5). Scale bars, 50 μm. (H and I) Representative flow cytometry plots (H) and quantification (I) results showing the frequencies of Annexin V^+ PLC/PRF/5 cells after sorafenib and huCAR T cell treatment. Before Annexin V staining, PLC/PRF/5 cells were prelabeled with Cell Trace Violet dye and then treated with huCAR T cells at a 1:10 ratio and various concentrations of sorafenib for 48 h. The results are expressed as the mean ± SEM. Significance of findings was defined as follows: ns, not significant; $p > 0.05$; *$p < 0.05$; **$p < 0.01$; ***$p < 0.001$.

combined mouse and huCAR T cells with the clinically accessible agent sorafenib. Although mouse and huCAR T cells showed different sensitivities to a pharmacologic dose of sorafenib, a subpharmacologic dose of sorafenib enhanced the antitumor activities of mouse and huCAR T cells, at least in part through macrophage modulation or apoptosis promotion. Our findings provide the basis for a clinical trial using a combination of sorafenib and GPC3-redirected CAR T cells against HCC.

MATERIALS AND METHODS

Primary Cells and Cell Lines

Hepa1-6 mouse HCC cells were purchased from the Chinese Academy of Sciences (Shanghai, China) and modified to express mouse GPC3, human GPC3, and chimeric GPC3 (chGPC3). The human HCC cell line PLC/PRF/5 was purchased from ATCC. All the HCC cell lines were cultivated in DMEM (Gibco) supplemented with 10% fetal bovine serum (FBS; GIBCO), penicillin (100 U/mL), and streptomycin (0.1 mg/mL).

BMDMs were generated as previously described.[45] Briefly, bone marrow flushed from femurs and tibias of mice were filtered through a 70 μm nylon cell strainer and plated in Petri dishes in DMEM supplemented with 10% heat-inactivated FBS, recombinant murine M-CSF (50 ng/mL; Peprotech), 2-mercaptoethanol (50 μM), penicillin (100 U/mL), and streptomycin (0.1 mg/mL). The cells were re-fed on day 3 and were used within 10 days.

Expression Constructs

The human-mouse GPC3 chimera (chGPC3) was built by replacing a sequence (Lys^{538} to Pro^{558}) in mouse GPC3 (GemBank: NM_016697.3) with a sequence from the 9F2-binding epitope (Ser^{539} to His^{559}) in human GPC3 (Genbank: NM_001164617.1). Then, chGPC3 was inserted into the third-generation, non-self-inactivating, EF-1a promoter-based lentiviral expression vector pWPT-eGFP. The CAR 9F2-m28z was composed of the anti-GPC3 scFv 9F2 linked by the hinge and transmembrane regions of the murine CD8α chain and intracellular murine CD28 and CD3ζ (mCD28-CD3z) signaling domains and was cloned into the *Eco*RI/*Sal*I sites of the retroviral vector MSCV-IRES-GFP for expression. The 9F2-hu28z construct has been described in detail by our laboratory.[46] The pCL-Eco retrovirus packaging vector and the MSCV-9F2-m28z cDNA expression vector were used to generate a retrovirus for murine T cell transduction. Lentiviruses and retroviruses were generated with a polyethylenimine-based DNA transfection system.

Generation of CAR T Cells

Mouse T cells were isolated from murine spleen using a mouse T cell isolation kit (Stemcell Technologies) and subsequently stimulated with anti-mouse CD3/CD28 magnetic beads (Invitrogen) for 24 h. Then, activated T cells were retrovirally transduced with 9F2-m28Z CAR in RetroNectin (Takara)-coated plates and cultivated in RPMI 1640 medium containing 10% heat-inactivated FBS, 2-mercaptoethanol (50 μM), recombinant human IL-2 (100 U/mL; Shanghai Huaxin High Biotech), penicillin (100 U/mL), and streptomycin (0.1 mg/mL). For generation of huCAR T cells, PBMCs obtained from Shanghai Blood Center were stimulated with anti-human CD3/CD28 magnetic beads (Invitrogen) for 48 h. Human T cells were then transduced with lentiviruses on RetroNectin-coated plates and maintained in culture in AIM-V (Gibco) supplemented with 2% human AB Serum (ABS; Gemini) and recombinant human IL-2 (500 U/mL).

Flow Cytometry

chGPC3 on Hepa1-6 cells was detected by mAb 9F2 followed by goat anti-mouse IgG-PE (Santa Cruz). To assess CAR expression, T cells were stained with a goat anti-human biotin-conjugated anti-Fab antibody (Jackson ImmunoResearch), followed by PE-conjugated streptavidin (eBioscience). For detection of CD107a and IFN-γ, T cells were fixed, permeabilized, and stained with antibodies against CD107a and IFN-γ (eBioscience). To analyze the *in vitro* proliferation of CAR T cells, a CellTrace Violet cell proliferation kit (Thermo Fisher Scientific) was used for labeling of cells to trace multiple generations via dye dilution by flow cytometry. For *in vivo* detection of CAR T cells prelabeled with CellTrace Violet dye, tumor tissues isolated from tumor-bearing mice were cut into small pieces and resuspended in digestion medium containing collagenase type IV (0.5 mg/mL; Sigma Aldrich) and DNase I (0.02 mg/mL; StemCell Technologies) for 30 min at 37°C on a shaker. Then, the suspension was filtered through a 70 μm Falcon cell strainer, centrifuged, and stained with antibodies against CD45 (BD Biosciences) and IFN-γ, according to the manufacturer's instructions.

Cytokine Release Assay

Mouse or huCAR T cells were cultivated in 24-well plates precoated with GPC3 protein for 24 h. The release of IL-2, IFN-γ, and TNF-α cytokines from activated mCAR or huCAR T cells was determined with a cytometric bead array (BD Biosciences), according to the manufacturer's instructions. The release of IL12 from BMDMs was detected with an ELISA kit (MultiSciences Biotechnology) as described in the manufacturer's instructions. For detection of IL12 within the tumor microenvironment, tumor tissues were dissected into small pieces, placed into normal saline, and homogenized with a TissueLyser (QIAGEN). After centrifugation, the supernatant of homogenates was collected and assayed for IL12 production with an ELISA kit.

Cytotoxicity Assay

GPC3-targeted mCAR or huCAR T cells were pretreated with sorafenib at different concentrations for 4 h and then incubated with Hepa1-6-chGPC3 or PLC/RPF/5 cells for 4 h. The specific cytotoxicity of GPC3-CAR T cells was evaluated with an LDH release assay using a CytoTox 96 nonradioactive cytotoxicity kit (Promega) according to the manufacturer's instructions.

Real-Time qPCR

TAMs were isolated from a single-cell suspension of sorafenib-treated Hepa1-6-chGPC3 tumors using anti-mouse F4/80 microbeads (Miltenyi Biotec). Total RNA was extracted from TAMs, and cDNAs were synthesized with a GoScript RT system (Promega). The relative gene expression of β-actin and IL12a was determined by using Real-Time

SYBR Green PCR Master Mix (Takara) on a 7500 Real-Time PCR System (Applied Biosystems). The primer sequences used were, forward primers: IL12, 5′-GCCAGGTGTCTTAGCCAGTC-3′ and Actin, 5′-ATCGTGCGTGACATCAAAGA-3′; reverse primers: IL12, AGC TCCCTCTTGTTGTGGAA-3′ and Actin, 5′-ACAGGATTCCATA CCCAAGAAG-3′. The delta-delta comparative threshold (ΔΔCt) method was used to calculate fold change in IL12a gene expression, which was normalized to actin as the reference gene.

IHC

Tumor tissues were fixed with formalin and embedded in paraffin. Then, 3-μm-thick sections were deparaffinized and treated with a heat-induced antigen retrieval citrate solution. Slides were then blocked with 1% BSA and stained with anti-human CD3ε antibody (Thermo Fisher Scientific), cleaved caspase-3 antibody (Cell Signaling Technology), or mAb 9F2 in the blocking solution overnight at 4°C. Secondary antibodies were added, and the results were visualized with a ChemMate Envision Detection Kit (DakoCytomation).

In Vivo Engraftment Model

All animals were treated under specific-pathogen-free conditions at the Experimental Animal Center of Shanghai Cancer Institute (Shanghai, China). All mouse studies were performed in accordance with protocols approved by the Shanghai Medical Experimental Animal Care Commission. Four- to 6-week-old C57BL/6 mice were injected with 1×10^7 Hepa1-6-chGPC3 cells in the right flank on day 0. Starting on day 8, 7.5 or 30 mg/kg sorafenib (Selleck) was administered orally to the mice for 10 days. On days 9 and 13, 2×10^6 CAR T cells were injected into the tail vein. To establish PLC/PRF/5 tumor models, 6-week-old NSG mice were inoculated subcutaneously with 5×10^6 PLC/PRF/5 cells on day 0. After 11 days, 7.5 or 30 mg/kg of sorafenib was administered by gavage daily for 2 weeks and with 2×10^6 CAR T cells injected intravenously.

Statistical Analysis

Statistical analyses were performed with GraphPad Prism software, version 7. One-way ANOVA and Tukey's test were performed to assess differences between groups treated with sorafenib at various concentrations. Tumor growth data were analyzed with two-way ANOVA. Survival curves were analyzed by using a log-rank test. All values and error bars represent the mean ± SEM. In the figures, significance of findings was defined as follows: ns, not significant; $p > 0.05$; *$p < 0.05$; **$p < 0.01$; or ***$p < 0.001$.

SUPPLEMENTAL INFORMATION

Supplemental Information can be found online at https://doi.org/10.1016/j.ymthe.2019.04.020.

AUTHOR CONTRIBUTIONS

Conception and design: Z.L. Development of methodology: X.W., H.J. Acquisition of data: X.W. and Hong Luo. Analysis and interpretation of data: X.W. and Hong Luo. Writing, review, and/or revision of the manuscript: Z.L., H.J., and X.W. Administrative, technical, or material support: B.S., S.D., R.S., Y.L., Hua Li, J.S. Study supervision: Z.L.

CONFLICTS OF INTEREST

Z.L. and X.W. are named co-inventors in patent applications relating to this work. Z.L. is a stockholder of CARsgen Therapeutics, Inc. The other authors declare no competing interests.

ACKNOWLEDGMENTS

This work was supported by funding from the "13th Five-Year Plan" National Science and Technology Major Project of China (2017ZX10203206006001), the National Natural Science Foundation of China (81872483 and 81871918), the Shanghai Municipal Commission of Health and Family Planning (20174Y0178), and a Grant-in-Aid for Young Scientists, Foundation of Shanghai Cancer Institute (SB18-05).

REFERENCES

1. Sadelain, M., Brentjens, R., and Rivière, I. (2013). The basic principles of chimeric antigen receptor design. Cancer Discov. *3*, 388–398.
2. Grupp, S.A., Kalos, M., Barrett, D., Aplenc, R., Porter, D.L., Rheingold, S.R., Teachey, D.T., Chew, A., Hauck, B., Wright, J.F., et al. (2013). Chimeric antigen receptor-modified T cells for acute lymphoid leukemia. N. Engl. J. Med. *368*, 1509–1518.
3. Porter, D.L., Levine, B.L., Kalos, M., Bagg, A., and June, C.H. (2011). Chimeric antigen receptor-modified T cells in chronic lymphoid leukemia. N. Engl. J. Med. *365*, 725–733.
4. Maude, S.L., Frey, N., Shaw, P.A., Aplenc, R., Barrett, D.M., Bunin, N.J., Chew, A., Gonzalez, V.E., Zheng, Z., Lacey, S.F., et al. (2014). Chimeric antigen receptor T cells for sustained remissions in leukemia. N. Engl. J. Med. *371*, 1507–1517.
5. Brudno, J.N., Maric, I., Hartman, S.D., Rose, J.J., Wang, M., Lam, N., Stetler-Stevenson, M., Salem, D., Yuan, C., Pavletic, S., et al. (2018). T Cells Genetically Modified to Express an Anti-B-Cell Maturation Antigen Chimeric Antigen Receptor Cause Remissions of Poor-Prognosis Relapsed Multiple Myeloma. J. Clin. Oncol. *36*, 2267–2280.
6. Ahmed, N., Brawley, V.S., Hegde, M., Robertson, C., Ghazi, A., Gerken, C., Liu, E., Dakhova, O., Ashoori, A., Corder, A., et al. (2015). Human Epidermal Growth Factor Receptor 2 (HER2) -Specific Chimeric Antigen Receptor-Modified T Cells for the Immunotherapy of HER2-Positive Sarcoma. J. Clin. Oncol. *33*, 1688–1696.
7. O'Rourke, D.M., Nasrallah, M.P., Desai, A., Melenhorst, J.J., Mansfield, K., Morrissette, J.J.D., Martinez-Lage, M., Brem, S., Maloney, E., Shen, A., et al. (2017). A single dose of peripherally infused EGFRvIII-directed CAR T cells mediates antigen loss and induces adaptive resistance in patients with recurrent glioblastoma. Sci. Transl. Med. *9*, a984.
8. Zhai, B., Shi, D., Gao, H., Qi, X., Jiang, H., Zhang, Y., et al. (2017). A phase I study of anti-GPC3 chimeric antigen receptor modified T cells (GPC3 CAR-T) in Chinese patients with refractory or relapsed GPC3+ hepatocellular carcinoma (r/r GPC3+ HCC). J. Clin. Oncol. *35* (*Suppl 15*), 3049.
9. Prieto, J., Melero, I., and Sangro, B. (2015). Immunological landscape and immunotherapy of hepatocellular carcinoma. Nat. Rev. Gastroenterol. Hepatol. *12*, 681–700.
10. Zhou, S.L., Zhou, Z.J., Hu, Z.Q., Huang, X.W., Wang, Z., Chen, E.B., Fan, J., Cao, Y., Dai, Z., and Zhou, J. (2016). Tumor-Associated Neutrophils Recruit Macrophages and T-Regulatory Cells to Promote Progression of Hepatocellular Carcinoma and Resistance to Sorafenib. Gastroenterology *150*, 1646–1658.e17.
11. Fu, J., Xu, D., Liu, Z., Shi, M., Zhao, P., Fu, B., Zhang, Z., Yang, H., Zhang, H., Zhou, C., et al. (2007). Increased regulatory T cells correlate with CD8 T-cell impairment and poor survival in hepatocellular carcinoma patients. Gastroenterology *132*, 2328–2339.
12. Long, A.H., Highfill, S.L., Cui, Y., Smith, J.P., Walker, A.J., Ramakrishna, S., El-Etriby, R., Galli, S., Tsokos, M.G., Orentas, R.J., and Mackall, C.L. (2016). Reduction of MDSCs with All-trans Retinoic Acid Improves CAR Therapy Efficacy for Sarcomas. Cancer Immunol. Res. *4*, 869–880.
13. Wang, X., Walter, M., Urak, R., Weng, L., Huynh, C., Lim, L., Wong, C.W., Chang, W.C., Thomas, S.H., Sanchez, J.F., et al. (2018). Lenalidomide Enhances the Function

of CS1 Chimeric Antigen Receptor-Redirected T Cells Against Multiple Myeloma. Clin. Cancer Res. *24*, 106–119.

14. Tang, L., Zheng, Y., Melo, M.B., Mabardi, L., Castaño, A.P., Xie, Y.Q., Li, N., Kudchodkar, S.B., Wong, H.C., Jeng, E.K., et al. (2018). Enhancing T cell therapy through TCR-signaling-responsive nanoparticle drug delivery. Nat. Biotechnol. *36*, 707–716.

15. SHARP Investigators Study Group (2008). Sorafenib in advanced hepatocellular carcinoma. N. Engl. J. Med. *359*, 378–390.

16. Wilhelm, S.M., Carter, C., Tang, L., Wilkie, D., McNabola, A., Rong, H., Chen, C., Zhang, X., Vincent, P., McHugh, M., et al. (2004). BAY 43-9006 exhibits broad spectrum oral antitumor activity and targets the RAF/MEK/ERK pathway and receptor tyrosine kinases involved in tumor progression and angiogenesis. Cancer Res. *64*, 7099–7109.

17. Wilhelm, S., Carter, C., Lynch, M., Lowinger, T., Dumas, J., Smith, R.A., Schwartz, B., Simantov, R., and Kelley, S. (2006). Discovery and development of sorafenib: a multikinase inhibitor for treating cancer. Nat. Rev. Drug Discov. *5*, 835–844.

18. Liu, L., Cao, Y., Chen, C., Zhang, X., McNabola, A., Wilkie, D., Wilhelm, S., Lynch, M., and Carter, C. (2006). Sorafenib blocks the RAF/MEK/ERK pathway, inhibits tumor angiogenesis, and induces tumor cell apoptosis in hepatocellular carcinoma model PLC/PRF/5. Cancer Res. *66*, 11851–11858.

19. Houben, R., Voigt, H., Noelke, C., Hofmeister, V., Becker, J.C., and Schrama, D. (2009). MAPK-independent impairment of T-cell responses by the multikinase inhibitor sorafenib. Mol. Cancer Ther. *8*, 433–440.

20. Zhao, W., Gu, Y.H., Song, R., Qu, B.Q., and Xu, Q. (2008). Sorafenib inhibits activation of human peripheral blood T cells by targeting LCK phosphorylation. Leukemia *22*, 1226–1233.

21. Chen, Y., Ramjiawan, R.R., Reiberger, T., Ng, M.R., Hato, T., Huang, Y., Ochiai, H., Kitahara, S., Unan, E.C., Reddy, T.P., et al. (2015). CXCR4 inhibition in tumor microenvironment facilitates anti-programmed death receptor-1 immunotherapy in sorafenib-treated hepatocellular carcinoma in mice. Hepatology *61*, 1591–1602.

22. Kalathil, S.G., Lugade, A.A., Miller, A., Iyer, R., and Thanavala, Y. (2016). PD-1^{+} and Foxp3^{+} T cell reduction correlates with survival of HCC patients after sorafenib therapy. JCI Insight *1*, e86182.

23. Chen, M.L., Yan, B.S., Lu, W.C., Chen, M.H., Yu, S.L., Yang, P.C., and Cheng, A.L. (2014). Sorafenib relieves cell-intrinsic and cell-extrinsic inhibitions of effector T cells in tumor microenvironment to augment antitumor immunity. Int. J. Cancer *134*, 319–331.

24. Edwards, J.P., and Emens, L.A. (2010). The multikinase inhibitor sorafenib reverses the suppression of IL-12 and enhancement of IL-10 by PGE_2 in murine macrophages. Int. Immunopharmacol. *10*, 1220–1228.

25. Sprinzl, M.F., Reisinger, F., Puschnik, A., Ringelhan, M., Ackermann, K., Hartmann, D., Schiemann, M., Weinmann, A., Galle, P.R., Schuchmann, M., et al. (2013). Sorafenib perpetuates cellular anticancer effector functions by modulating the crosstalk between macrophages and natural killer cells. Hepatology *57*, 2358–2368.

26. Sunay, M.M.E., Foote, J.B., Leatherman, J.M., Edwards, J.P., Armstrong, T.D., Nirschl, C.J., Hicks, J., and Emens, L.A. (2017). Sorafenib combined with HER-2 targeted vaccination can promote effective T cell immunity in vivo. Int. Immunopharmacol. *46*, 112–123.

27. Yang, Y., Jiang, H., Gao, H., Kong, J., Zhang, P., Hu, S., Shi, B., Zhang, P., Yao, M., and Li, Z. (2012). The monoclonal antibody CH12 enhances the sorafenib-mediated growth inhibition of hepatocellular carcinoma xenografts expressing epidermal growth factor receptor variant III. Neoplasia *14*, 509–518.

28. Motoshima, T., Komohara, Y., Horlad, H., Takeuchi, A., Maeda, Y., Tanoue, K., Kawano, Y., Harada, M., Takeya, M., and Eto, M. (2015). Sorafenib enhances the antitumor effects of anti-CTLA-4 antibody in a murine cancer model by inhibiting myeloid-derived suppressor cells. Oncol. Rep. *33*, 2947–2953.

29. Gao, H., Li, K., Tu, H., Pan, X., Jiang, H., Shi, B., Kong, J., Wang, H., Yang, S., Gu, J., and Li, Z. (2014). Development of T cells redirected to glypican-3 for the treatment of hepatocellular carcinoma. Clin. Cancer Res. *20*, 6418–6428.

30. Shultz, L.D., Lyons, B.L., Burzenski, L.M., Gott, B., Chen, X., Chaleff, S., Kotb, M., Gillies, S.D., King, M., Mangada, J., et al. (2005). Human lymphoid and myeloid cell development in NOD/LtSz-scid IL2R gamma null mice engrafted with mobilized human hemopoietic stem cells. J. Immunol. *174*, 6477–6489.

31. Brentjens, R.J., Davila, M.L., Riviere, I., Park, J., Wang, X., Cowell, L.G., Bartido, S., Stefanski, J., Taylor, C., Olszewska, M., et al. (2013). CD19-targeted T cells rapidly induce molecular remissions in adults with chemotherapy-refractory acute lymphoblastic leukemia. Sci. Transl. Med. *5*, 177ra38.

32. Joseph, R.W., Elassaiss-Schaap, J., Kefford, R., Hwu, W., Wolchok, J.D., Joshua, A.M., Ribas, A., Hodi, F.S., Hamid, O., Robert, C., Daud, A., et al. (2018). Baseline Tumor Size Is an Independent Prognostic Factor for Overall Survival in Patients with Melanoma Treated with Pembrolizumab. Clin. Cancer Res. *24*, 4960–4967.

33. Adachi, K., Kano, Y., Nagai, T., Okuyama, N., Sakoda, Y., and Tamada, K. (2018). IL-7 and CCL19 expression in CAR-T cells improves immune cell infiltration and CAR-T cell survival in the tumor. Nat. Biotechnol. *36*, 346–351.

34. Hegde, M., Mukherjee, M., Grada, Z., Pignata, A., Landi, D., Navai, S.A., Wakefield, A., Fousek, K., Bielamowicz, K., Chow, K.K., et al. (2016). Tandem CAR T cells targeting HER2 and IL13Rα2 mitigate tumor antigen escape. J. Clin. Invest. *126*, 3036–3052.

35. Chuang, H.Y., Chang, Y.F., Liu, R.S., and Hwang, J.J. (2014). Serial low doses of sorafenib enhance therapeutic efficacy of adoptive T cell therapy in a murine model by improving tumor microenvironment. PLoS ONE *9*, e109992.

36. Hipp, M.M., Hilf, N., Walter, S., Werth, D., Brauer, K.M., Radsak, M.P., Weinschenk, T., Singh-Jasuja, H., and Brossart, P. (2008). Sorafenib, but not sunitinib, affects function of dendritic cells and induction of primary immune responses. Blood *111*, 5610–5620.

37. Awada, A., Hendlisz, A., Gil, T., Bartholomeus, S., Mano, M., de Valeriola, D., Strumberg, D., Brendel, E., Haase, C.G., Schwartz, B., and Piccart, M. (2005). Phase I safety and pharmacokinetics of BAY 43-9006 administered for 21 days on/7 days off in patients with advanced, refractory solid tumours. Br. J. Cancer *92*, 1855–1861.

38. Strumberg, D., Richly, H., Hilger, R.A., Schleucher, N., Korfee, S., Tewes, M., Faghih, M., Brendel, E., Voliotis, D., Haase, C.G., et al. (2005). Phase I clinical and pharmacokinetic study of the Novel Raf kinase and vascular endothelial growth factor receptor inhibitor BAY 43-9006 in patients with advanced refractory solid tumors. J. Clin. Oncol. *23*, 965–972.

39. Federico, A., Orditura, M., Cotticelli, G., DE Sio, I., Romano, M., Gravina, A.G., Dallio, M., Fabozzi, A., Ciardiello, F., Loguercio, C., and DE Vita, F. (2015). Safety and efficacy of sorafenib in patients with advanced hepatocellular carcinoma and Child-Pugh A or B cirrhosis. Oncol. Lett. *9*, 1628–1632.

40. Hu, S., Niu, H., Inaba, H., Orwick, S., Rose, C., Panetta, J.C., Yang, S., Pounds, S., Fan, Y., Calabrese, C., et al. (2011). Activity of the multikinase inhibitor sorafenib in combination with cytarabine in acute myeloid leukemia. J. Natl. Cancer Inst. *103*, 893–905.

41. Pawaskar, D.K., Straubinger, R.M., Fetterly, G.J., Hylander, B.H., Repasky, E.A., Ma, W.W., and Jusko, W.J. (2013). Physiologically based pharmacokinetic models for everolimus and sorafenib in mice. Cancer Chemother. Pharmacol. *71*, 1219–1229.

42. Newick, K., O'Brien, S., Moon, E., and Albelda, S.M. (2017). CAR T Cell Therapy for Solid Tumors. Annu. Rev. Med. *68*, 139–152.

43. Hirayama, A.V., Gauthier, J., Hay, K.A., Voutsinas, J.M., Wu, Q., Gooley, T., Li, D., Cherian, S., Chen, X., Pender, B.S., et al. (2019). The response to lymphodepletion impacts PFS in aggressive non-Hodgkin lymphoma patients treated with CD19 CAR-T cells. Blood *133*, 2011–2018.

44. Rosenberg, S.A., Restifo, N.P., Yang, J.C., Morgan, R.A., and Dudley, M.E. (2008). Adoptive cell transfer: a clinical path to effective cancer immunotherapy. Nat. Rev. Cancer *8*, 299–308.

45. Trouplin, V., Boucherit, N., Gorvel, L., Conti, F., Mottola, G., and Ghigo, E. (2013). Bone marrow-derived macrophage production. J. Vis. Exp. *81*, e50966.

46. Yu, M., Luo, H., Fan, M., Wu, X., Shi, B., Di, S., Liu, Y., Pan, Z., Jiang, H., and Li, Z. (2018). Development of GPC3-Specific Chimeric Antigen Receptor-Engineered Natural Killer Cells for the Treatment of Hepatocellular Carcinoma. Mol. Ther. *26*, 366–378.

YMTHE, Volume *27*

Supplemental Information

Combined Antitumor Effects of Sorafenib and GPC3-CAR T Cells in Mouse Models of Hepatocellular Carcinoma

Xiuqi Wu, Hong Luo, Bizhi Shi, Shengmeng Di, Ruixin Sun, Jingwen Su, Ying Liu, Hua Li, Hua Jiang, and Zonghai Li

Supplemental Figures

Supplementary Figure S1:

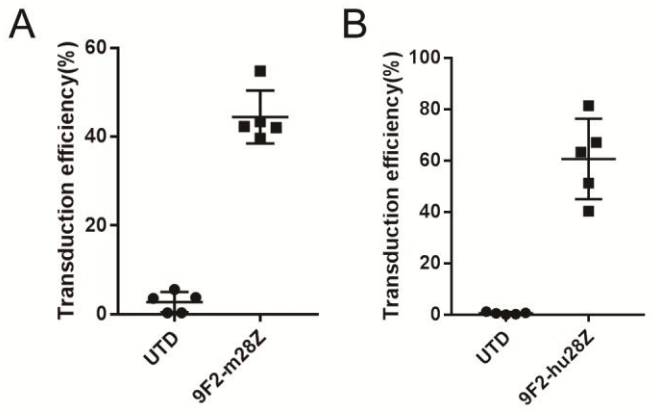

Supplementary Figure S1: Transduction efficiencies of murine and human CAR T cells. (A) Mouse T cells were transduced by 9F2-m28Z with positive rate as 45% on average. (B) Human T cells were transduced by 9F2-hu28Z with positive rate as 60% on average. The results are expressed as the mean ± SEM.

Supplementary Figure S2:

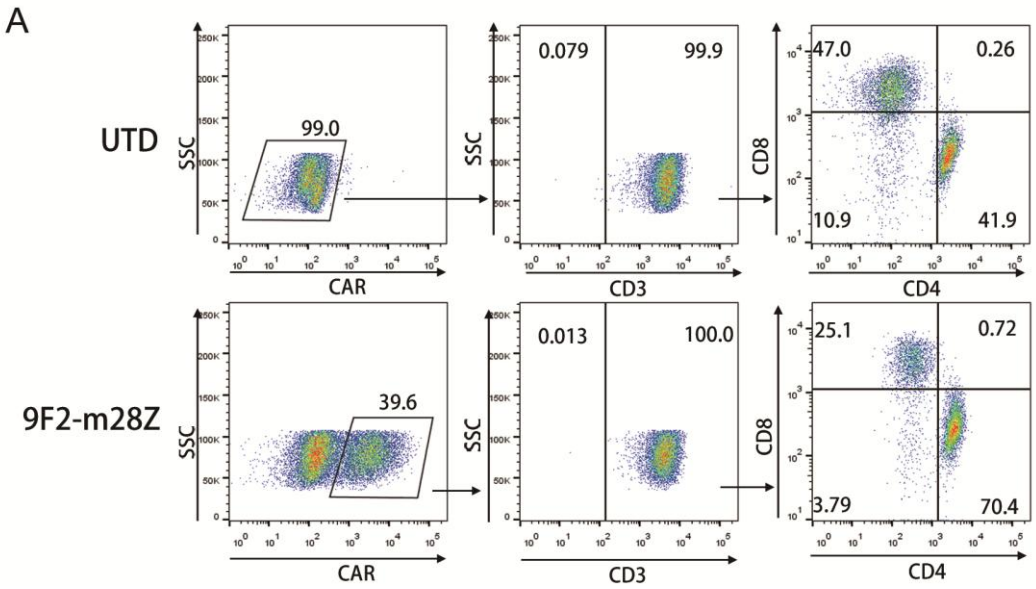

Supplementary Figure S2: Basic phenotypes of murine CAR T cells. (A) A representative flow cytometry analysis of CD3, CD4, CD8 expression on untransduced (UTD) mouse T cells and mCAR T cells transduced with 9F2-m28Z.

Supplementary Figure S3:

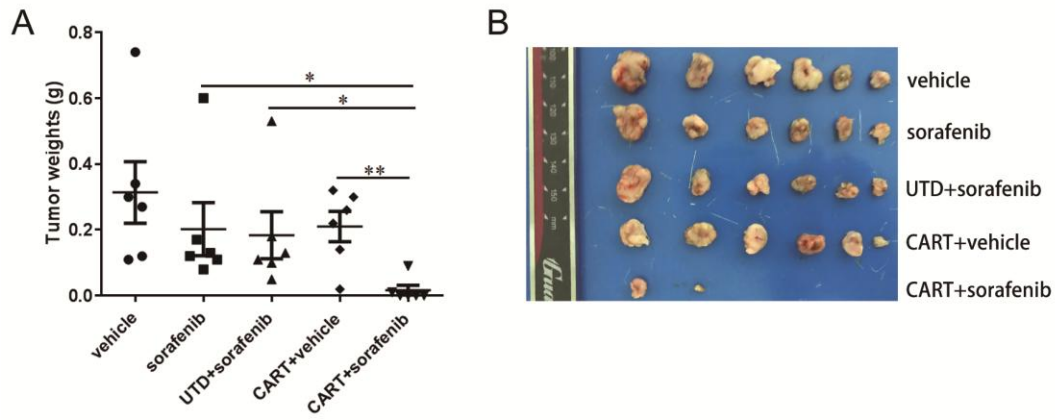

Supplementary Figure S3: Tumor samples after sorafenib and CAR T cell treatment. On day 28 after the last determination, mice were euthanized. Then, tumor weight was measured (A) and tumor samples were exhibited in (B). The results are expressed as the mean ± SEM. Significance of findings was defined as follows: ns, not significant; $p > 0.05$; *$p < 0.05$; **$p < 0.01$; or ***$p < 0.001$.

Supplementary Figure S4:

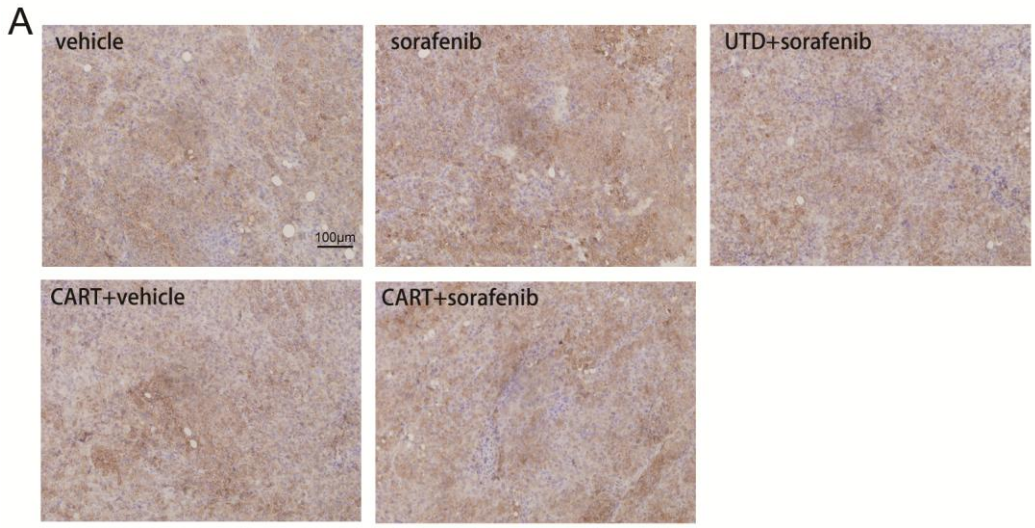

Supplementary Figure S4: chGPC3 expression within tumor samples after sorafenib and CAR T cell treatment. (A) Representative immunostaining images of chGPC3 expression in tumor tissues. Scale bars, 100μM.

Supplementary Figure S5:

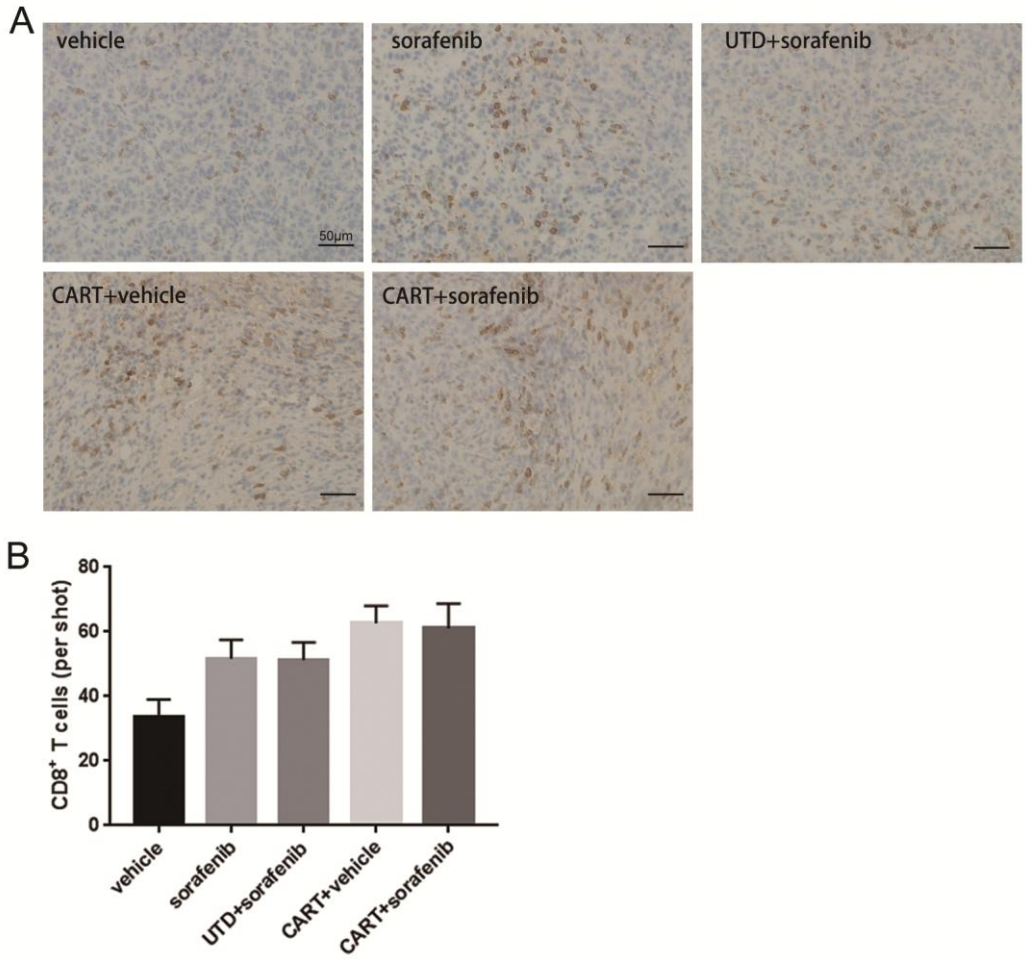

Supplementary Figure S5: Representative images of CD8+ mouse T cell infiltration in tumor tissues. (A) Representative images of $CD8^+$ mouse T cell infiltration in tumor tissues as detected by immunohistochemistry staining. Scale bars, 50μM. (B) Quantification of $CD8^+$ mouse T cell infiltration in tumor tissues (n=5). The results are expressed as the mean ± SEM.

Supplementary Figure S6:

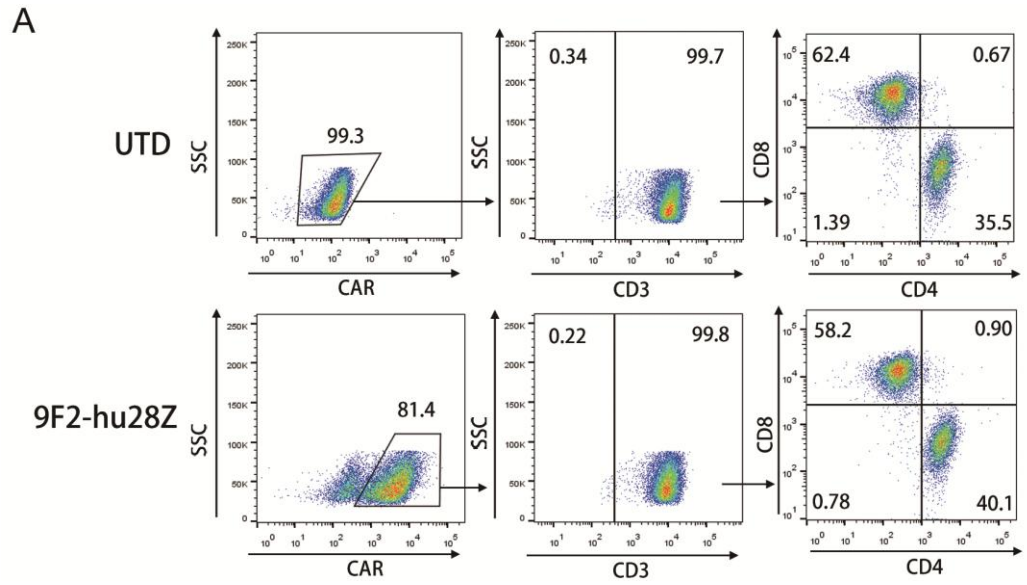

Supplementary Figure S6: Basic phenotypes of human CAR T cells. (A) A representative flow cytometry analysis of CD3, CD4, CD8 expression on untransduced (UTD) human T cells and huCAR T cells transduced with 9F2-hu28Z.

Supplementary Figure S7:

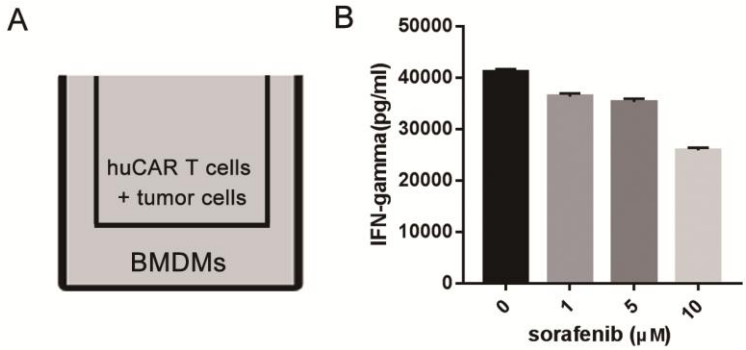

Supplementary Figure S7: Sorafenib-treated BMDMs did not enhance the function of huCAR T cells in vitro. (A and B) Transwell co-culture of huCAR T cells with BMDMs. BMDMs were treated with sorafenib and LPS (10 ng/mL) for 8 hours. Then huCAR T cells and tumor cells were added into the upper chamber for another 16h co-culture with sorafenib-treated BMDMs. IFN-γ expression in supernatants were assayed by cytometric bead array (CBA). Data reflects mean ± SD of triplicate wells.

Supplementary Figure S8:

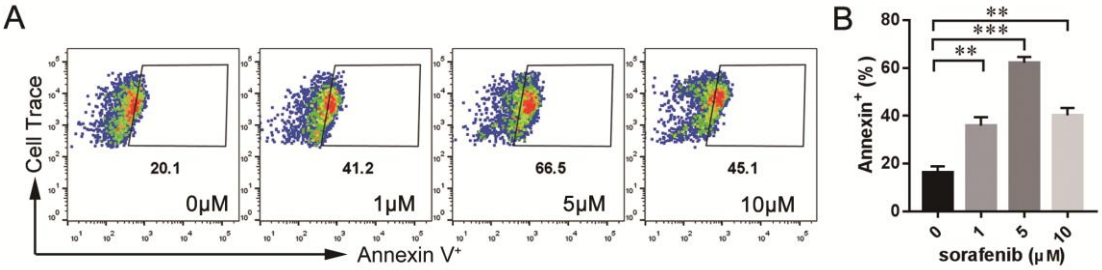

Supplementary Figure S8: Apoptosis of Hepa1-6-chGPC3 cells was significantly increased when mCAR T cells were combined with sorafenib. (A and B) Representative flow cytometry plots and quantification results showing the frequencies of Annexin V^+ Hepa1-6-chGPC3 cells after sorafenib and mCAR T cells treatment. Before Annexin V Staining, Hepa1-6-chGPC3 cells were pre-labeled with Cell Trace Violet dye and then treated with mCAR T cells at 1: 10 ratio and various concentrations of sorafenib for 24h. Results are expressed as mean ± SEM of triplicates. Significance of findings was defined as follows: ns, not significant; $p > 0.05$; *$p < 0.05$; **$p < 0.01$; or ***$p < 0.001$.